

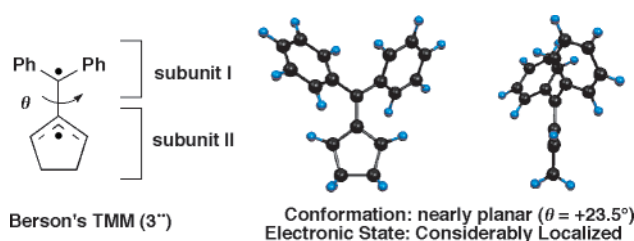
An Evolved Explanation for the Molecular Geometry and Electronic Structure of Diphenyl-Substituted Cyclic Trimethylenemethane in the Ground State: A Nearly Planar Conformation with a Considerably Localized Electronic State

Hiroshi Ikeda,* Hayato Namai, Hirotsugu Taki, and Tsutomu Miyashi

Department of Chemistry, Graduate School of Science, Tohoku University, Sendai 980-8578, Japan

iked@org.chem.tohoku.ac.jp

Received November 26, 2004



We reinvestigated the molecular geometry and electronic structure of the diphenyl-substituted, five-membered cyclic trimethylenemethane (TMM) diradical (Berson's TMM, 3^{**}) using UV/VIS absorption and emission spectroscopy combined with density functional theory (DFT) and time-dependent (TD)-DFT calculations. Two intense absorption bands, A and B, with λ_{ab} at 298 and 328 nm, respectively, a weak absorption band C, with λ_{ab} at 472 nm, and an intense emission band D, with λ_{em} at 491 nm, were observed for 3^{**} . By comparing the spectrum of 3^{**} with those of the 1,1-diphenylethyl (7^{\bullet}) and cyclopent-2-en-1-yl (9^{\bullet}) radicals, it was found that bands B, C, and D originated from the diphenylmethyl radical moiety (subunit I), while band A should most likely be assigned to an electronic transition related to an interaction between subunit I and residual subunit II, the cyclopentenyl radical moiety. An UB3LYP/cc-pVDZ calculation indicated that, in the ground state, the two unpaired electrons of 3^{**} are mainly localized in subunits I and II, respectively, and the interaction between them is inefficient, despite the nearly planar conformation ($\theta = +23.5^\circ$). Furthermore, a TD-UB3LYP/cc-pVDZ calculation suggested that absorption band A is assigned to an electronic transition involved with enhancement of the electron density of the C-2–C-3 bond. Substituent effects on the absorption and emission spectra of 3^{**} using 11^{**} and 13^{**} support the conclusion based on the experiments and calculations. Therefore, we propose an evolved explanation for the molecular geometry and electronic structure of the ground state of 3^{**} in a low-temperature matrix, a nearly planar conformation with a considerably localized electronic state, which alone accounts for the spectroscopic characteristics.

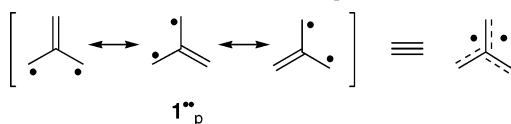
Introduction

The parent trimethylenemethane (TMM, 1^{\bullet}_p in Chart 1) and its derivatives are the most fundamental and commonly quoted representatives of non-Kekulé molecules, and have attracted much attention during the last few decades,¹ following Moffitt's theoretical prediction of their unique electronic structure.² Dowd was the first to observe the parent prototype 1^{\bullet}_p and its triplet multiplicity by ESR using 4-methylene-1-pyrazoline.³ A milestone in this field, achieved by Berson and co-workers, was the development of a new versatile route to a number of substituted, five-membered cyclic TMMs. This allowed

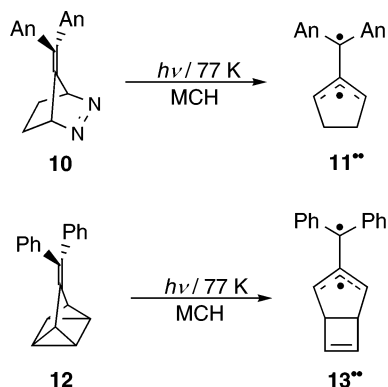
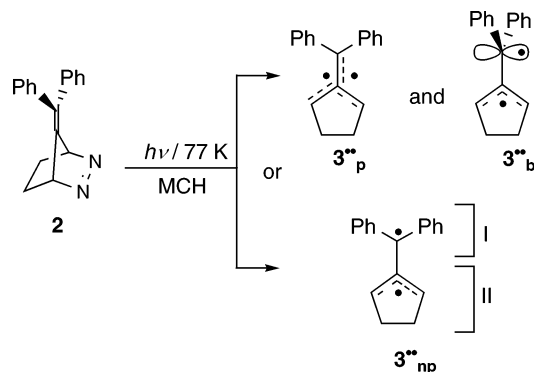
not only energetic study and detailed investigation of chemical reactivity, but also successful observations of

(1) For books or recent experimental reviews for TMMs, see: (a) Berson, J. A. In *Rearrangements in Ground and Excited States*; Mayo, P. d., Ed.; Academic: New York, 1980; Vol. 1, pp 311–390. (b) Borden, W. T., Ed.; *Diradicals*; Borden, W. T., Ed.; John Wiley & Sons: New York, 1982; pp 1–72. (c) Berson, J. A. In *Diradicals*; Borden, W. T., Ed.; John Wiley & Sons: New York, 1982; pp 151–194. (d) Berson, J. A. In *Reactive Intermediate Chemistry*; Moss, R. A., Platz, M. S., Jones, M., Eds.; John Wiley & Sons: Hoboken, 2004; pp 165–203. (e) Little, R. D. *Chem. Rev.* **1996**, *96*, 93–114. (f) Allan, A. K.; Carroll, G. L.; Little, R. D. *Eur. J. Org. Chem.* **1998**, 1–12. (g) Nakamura, E.; Yamago, S. *Acc. Chem. Res.* **2002**, *35*, 867–877.

(2) Moffitt, W. E., cited in: Coulson, C. A. *J. Chim. Phys. Physicochim. Biol.* **1948**, *45*, 243–248.

CHART 1. The Parent TMM (1^{**p})^a

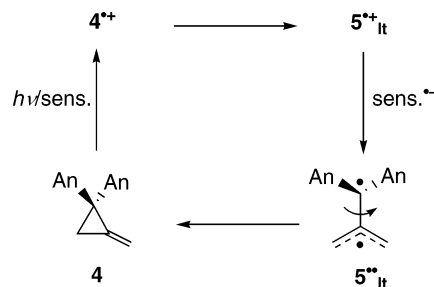
^a Abbreviation: subscript p, planar structure.

SCHEME 1^a

^a Abbreviations: MCH, methylcyclohexane; An, 4-MeOC₆H₄; subscripts b and np, bisected and nearly planar structures, respectively.

ESR, UV/VIS absorption, and emission spectra.⁴ Having photolyzed 7-(diphenylmethylene)-2,3-diazabicyclo[2.2.1]hept-2-ene (**2**) in a methylcyclohexane (MCH) matrix at 77 K, Turro, Berson, and Platz observed the characteristic absorption ($\lambda_{ab} = 299, 315, 329, 440,$ and 480 nm) and emission ($\lambda_{em} = 488$ and 512 nm) spectra of the diphenyl-substituted, five-membered cyclic TMM (**3**** in Scheme 1).^{4c}

To interpret the observed spectra, they considered two rationales that they refer to as the “single and two molecular species postulates”.^{4c} Although both postulates leave unanswered questions, they preferred the latter: two species in thermal equilibrium associated with the absorption and emission spectra.⁵ As shown in Scheme 1, one species was the more stable planar conformer, **3**_p**, in the ground state, like the parent TMM,⁶ which would

SCHEME 2^a

^a Abbreviation: sens., sensitizer; lt, largely twisted.

contribute to the absorption bands with λ_{ab} at 299, 315, and 329 nm, but not to any emission bands. A metastable bisected structure **3**_b** is the other one, which would contribute to the absorption bands with λ_{ab} at 440 and 480 nm and the emission bands with λ_{em} at 488 and 512 nm. They assumed one-way conversion from the excited state of **3**_p** to that of **3**_b**. However, unanswered questions remained, particularly as to energetics, and the molecular geometry and electronic structure of **3**** has not been thoroughly elucidated.

We recently reported⁷ that a photoinduced electron-transfer methylenecyclopropane rearrangement of 2,2-bis(4-methoxyphenyl)-1-methylenecyclopropane (**4**) involves a TMM radical cation, **5**+_{lt}**, and the corresponding TMM diradical, **5**+_{lt}** (Scheme 2). Spectroscopic results of Chemically Induced Dynamic Nuclear Polarization (CIDNP), time-resolved absorption, and ESR [Chemically Induced Dynamic Electron Polarization (CIDEP)] spectroscopy on laser flash photolysis at room temperature suggested that **5**+_{lt}** is largely twisted in the ground state, in striking contrast to the previous postulate^{4c} for **3****. The confusion and controversy surrounding the molecular geometry and electronic structure of substituted TMMs,⁸ especially aryl-substituted derivatives,⁹ led us to make further investigations.

To gain insight into the molecular geometry and electronic structure of **3****, we compared the spectra of **3**** with those of structurally related radicals and TMMs in

(5) Later studies of the Berson group demonstrated that the single molecular species postulate was actually correct. For the details, see the Conclusion.

(6) (a) Yarkony, D. R.; Schaefer, H. F., III *J. Am. Chem. Soc.* **1974**, *96*, 3754–3758. (b) Davidson, E. R.; Borden, W. T. *J. Phys. Chem.* **1976**, *64*, 663–666. (c) Davis, J. H.; Goddard, W. A., III *J. Am. Chem. Soc.* **1977**, *99*, 4242–4247. (d) Dixon, D. A.; Foster, R.; Halgren, T. A.; Lipscomb, W. N. *J. Am. Chem. Soc.* **1978**, *100*, 1359–1365. (e) Auster, S. B.; Pitzer, R. M.; Platz, M. S. *J. Am. Chem. Soc.* **1982**, *104*, 3812–3815. (f) Slipchenko, L. V.; Krylov, A. I. *J. Chem. Phys.* **2003**, *118*, 6874–6883.

(7) (a) Miyashi, T.; Takahashi, Y.; Mukai, T.; Roth, H. D.; Schilling, M. L. *J. Am. Chem. Soc.* **1985**, *107*, 1079–1080. (b) Ikeda, H.; Nakamura, T.; Miyashi, T.; Goodman, J. L.; Akiyama, K.; Tero-Kubota, S.; Houmam, A.; Wayner, D. D. M. *J. Am. Chem. Soc.* **1998**, *120*, 5832–5833. (c) Ikeda, H.; Akiyama, K.; Takahashi, Y.; Nakamura, T.; Ishizaki, S.; Shiratori, Y.; Ohaku, H.; Goodman, J. L.; Houmam, A.; Wayner, D. D. M.; Tero-Kubota, S.; Miyashi, T. *J. Am. Chem. Soc.* **2003**, *125*, 9147–9157.

(8) (a) Berson, J. A.; Corwin, L. R.; Davis, J. H. *J. Am. Chem. Soc.* **1974**, *96*, 6117–6179. (b) Crawford, R. J.; Tokunaga, H.; Schrijver, L. M. H. C.; Godard, J. C. *Can. J. Chem.* **1978**, *56*, 998–1004. (c) Cichra, D. A.; Duncan, C. D.; Berson, J. A. *J. Am. Chem. Soc.* **1980**, *102*, 6527–6533.

(9) (a) Roth, W. R.; Winzer, M.; Lennartz, H.-W.; Boese, R. *Chem. Ber.* **1993**, *126*, 2717–2725. (b) Abe, M.; Adam, W. *J. Chem. Soc., Perkin Trans. 2* **1998**, 1063–1068. (c) Roth, W. R.; Wildt, H.; Schlenker, A. *Eur. J. Org. Chem.* **2001**, 4081–4099.

(3) Dowd, P. *J. Am. Chem. Soc.* **1966**, *88*, 2587–2589.

(4) (a) Berson, J. A.; Bushby, R. J.; McBride, J. M.; Tremelling, M. *J. Am. Chem. Soc.* **1971**, *93*, 1544–1546. (b) Platz, M. S.; McBride, J. M.; Little, R. D.; Harrison, J. J.; Shaw, A.; Potter, S. E.; Berson, J. A. *J. Am. Chem. Soc.* **1976**, *98*, 5725–5726. (c) Turro, N. J.; Mirbach, M. J.; Harrit, N.; Berson, J. A.; Platz, M. S. *J. Am. Chem. Soc.* **1978**, *100*, 7653–7658. (d) Berson, J. A. *Acc. Chem. Res.* **1978**, *11*, 446–453.

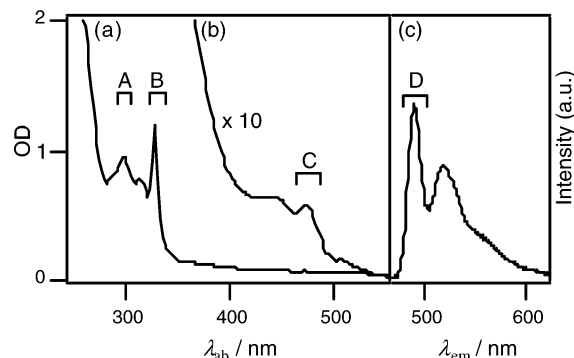
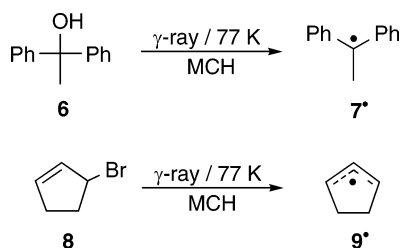


FIGURE 1. (a and b) UV/VIS absorption and (c) emission ($\lambda_{\text{ex}} = 328$ nm, band-pass 5 nm) spectra of **3**** generated by the photolysis of **2** (1.0 mM) in an MCH glassy matrix at 77 K for (a) 2 min and (b and c) 10 min.

SCHEME 3



low-temperature matrices, and conducted a density functional theory (DFT) calculation. The DFT calculation and comparison of the UV/VIS absorption and emission spectra of **3**** with those of the 1,1-diphenylethyl (**7***, Scheme 3)¹⁰ and cyclopent-2-en-1-yl (**9***)¹¹ radicals implied that the ground-state TMM **3**** has a nearly planar structure (dihedral angle, $\theta = +23.5^\circ$, see Figure 3), but possesses an electronic state that is considerably localized in subunits I and II (**3**_{np}**), as shown in Scheme 1. A time-dependent (TD)-DFT calculation successfully reproduced the observed spectra. Substituent effects on the absorption and emission wavelengths found by using 7-[bis(4-methoxyphenyl)methylene]-2,3-diazabicyclo[2.2.1]hept-2-ene (**10**) and 3-benzhydrylidenequadricyclane (**12**)¹² support this explanation. Herein, we report an evolved explanation for the molecular geometry and electronic structure of the ground state **3**** in low-temperature matrix.

Results and Discussion

UV/VIS Absorption and Emission Spectra of **3**, **7***, and **9*** in MCH Matrices at 77 K.** According to the method of Berson and co-workers,^{4c} a MCH glassy matrix of diazene **2** (1.0 mM) was photolyzed with a Rayonet lamp (RUL-2537 Å, 15 W) for 2–10 min at 77 K. As shown in Figure 1 and summarized in Table 1, the resulting **3**** has intense absorption bands with λ_{ab} at 298, 316, and 328 nm, weak absorption bands with λ_{ab} at 448

TABLE 1. Experimental Absorption (λ_{ab}) and Emission Wavelengths (λ_{em}) in MCH Glassy Matrices at 77 K, and Calculated Electronic Transition Wavelengths (λ_{et}) of **3****, **7***, **11****, and **13****

species	$\lambda_{\text{ab}} / \text{nm}$			$\lambda_{\text{em}} / \text{nm}$			$\lambda_{\text{et}} / \text{nm}$		
3**	298 ^a	316	328 ^b	448	472 ^c	491 ^d	519	303 ^e	323 ^e
								(0.25 ^f)	(0.21 ^f)
7*		326	336	488	518	522	551		327 ^e
									(0.46 ^f)
11**	314	332	346	^g	494	ca. 510 ^h	^g	ⁱ	ⁱ
13**	310	316	328	452	472	488	515	ⁱ	ⁱ

^a Band A. ^b Band B. ^c Band C. ^d Band D. ^e Calculations were carried out with TD-UB3LYP/cc-pVDZ//UB3LYP/cc-pVDZ. ^f Calculated oscillator strengths (^f). ^g A broad (shoulder) absorption or emission band was observed. ^h See ref 15. ⁱ Not defined.

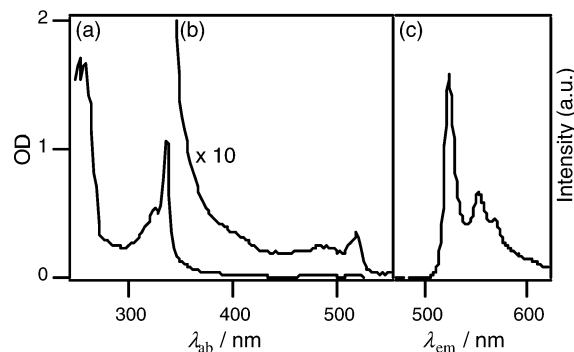


FIGURE 2. (a and b) UV/VIS absorption and (c) emission spectra ($\lambda_{\text{ex}} = 336$ nm, band-pass 5 nm) of **7*** generated by the γ -ray radiolysis of **6** (10 mM) in a MCH glassy matrix at 77 K.

and 472 nm, and intense emission bands with λ_{em} at 491 and 519 nm ($\lambda_{\text{ex}} = 328$ nm, band-pass 5 nm), in good agreement with a previous report.^{4c} The excitation spectrum ($\lambda_{\text{ex}} = 250$ –550 nm, $\lambda_{\text{em}} = 491$ nm) essentially corresponds to the absorption spectrum. We focused our investigation on the three absorption bands with λ_{ab} at 298 (band A), 328 (band B), and 472 nm (band C) and the emission band with λ_{em} at 491 nm (band D).¹³

For comparison purposes, the absorption and emission spectra of two skeletal subunits, viz. the diphenylethyl radical **7*** and the cyclopentenyl radical **9***, were generated at 77 K by γ -ray irradiation of MCH glassy matrices of 1,1-diphenylethanol (**6**, 10 mM) and 3-bromocyclopentene (**8**, 10 mM), respectively (Scheme 3). As shown in Figure 2 and listed in Table 1, radical **7*** had absorption bands with λ_{ab} at 326,¹³ 336, 488, and 518 nm and emission bands with λ_{em} at 522 and 551 nm ($\lambda_{\text{ex}} = 336$ nm, band-pass 5 nm), which corresponded to the respective bands of **3****, except band A, although the bands were somewhat red-shifted. As in the case of **3****, the excitation spectrum ($\lambda_{\text{ex}} = 250$ –550 nm, $\lambda_{\text{em}} = 522$ nm) of **7*** was essentially identical with its absorption spectrum. By contrast, **9*** did not exhibit any significant absorption or emission in the 250–600 nm region, although **9*** was definitely detected by ESR. These results strongly suggest that the ground state **3**** possesses an electronic state that is considerably localized in subunits I and II (see **3**_{np}** in Scheme 1), and that the three bands of **3**** (B, C,

(10) (a) Bromberg, A.; Meisel, D. *J. Phys. Chem.* **1985**, *89*, 2507–2513. (b) Bromberg, A.; Schmidt, K. H.; Meisel, D. *J. Am. Chem. Soc.* **1985**, *107*, 83–91.

(11) Rhodes, C. J. *J. Chem. Soc., Faraday Trans.* **1991**, *87*, 3179–3184.

(12) (a) Hirano, T.; Kumagai, T.; Miyashi, T.; Akiyama, K.; Ikegami, Y. *J. Org. Chem.* **1991**, *56*, 1907–1914. (b) Hirano, T.; Kumagai, T.; Miyashi, T.; Akiyama, K.; Ikegami, Y. *J. Org. Chem.* **1992**, *57*, 876–882.

(13) The 316-nm transition of **3**** and the 326-nm transition of **7*** are probably due to vibrational structures. Similar absorption bands attributable to vibrational structures are reported for the benzyl radical.¹⁴

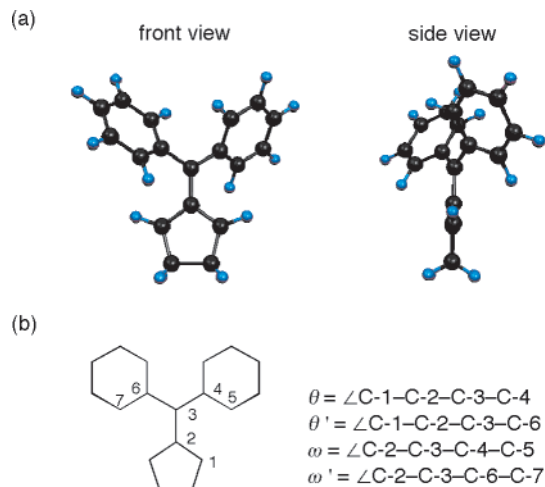


FIGURE 3. (a) Optimized geometry of 3^{**} with UB3LYP/cc-pVDZ. (b) Atom notation and definition of the dihedral angles (θ , θ' , ω , and ω') of 3^{**} .

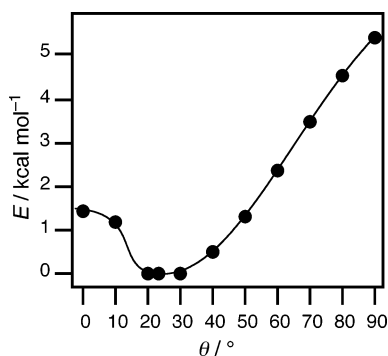


FIGURE 4. Potential energy (E) curve of 3^{**} along the dihedral angle (θ) calculated by UB3LYP/cc-pVDZ.

and D) originate from subunit I. However, the assignment of band A of 3^{**} remains uncertain, since neither of the single radicals 7^{\bullet} or 9^{\bullet} possessed an absorption band that corresponded to band A. The possible origin of band A is discussed later (vide infra).

DFT and TD-DFT Calculations of 3^{} and 7^{\bullet} :** We performed DFT and TD-DFT calculations on 3^{**} and 7^{\bullet} to further investigate the molecular geometry and electronic structure of the triplet state of 3^{**} . Figure 3a shows a representation of the optimized geometry of 3^{**} with UB3LYP/cc-pVDZ. The dihedral angles, θ and θ' , of C-1-C-2-C-3-C-4 and C-1-C-2-C-3-C-6 (Figure 3b) were optimized to be $+23.5^\circ$ (Figure 4) and -156.4° , respectively, while similar angles, ω and ω' , of C-2-C-3-C-4-C-5 and C-2-C-3-C-6-C-7 were calculated to be $+37.2^\circ$ and $+36.8^\circ$, respectively. These findings, especially θ and θ' , suggest that the ground state of 3^{**} is neither completely planar, like the parent TMM 1^{*p} , nor largely twisted, like 5^{*t} , but is nearly planar. The C-2-C-3 bond length ($d_{C-2-C-3}$) of the optimized 3^{**} ($\theta = +23.5^\circ$) was calculated to be 1.45 Å. As shown in Figure 5, $d_{C-2-C-3}$ of 3^{**} monotonically increased from 1.44(2) Å to 1.48(1) Å as θ varied from 0° to 90° .¹⁶ Note that these $d_{C-2-C-3}$ values are close to the C-C bond length ($d_{C-C} = 1.47$ Å)

(14) Ward, B. *Spectrochim. Acta* **1968**, *24A*, 813–818.

(15) An apparent emission maximum was observed at 544 nm. See the Supporting Information.

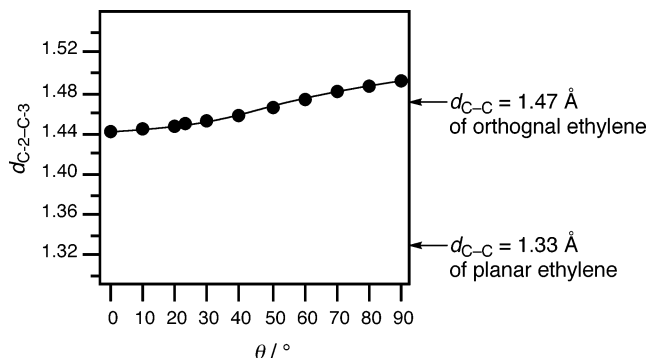


FIGURE 5. Dihedral angle (θ)-dependent changes of the C-2-C-3 bond length ($d_{C-2-C-3}$) calculated by UB3LYP/cc-pVDZ.

of the orthogonal ethylene, but longer than that (1.33 Å) of the planar ethylene.¹⁷ Therefore, twisting of the C-2-C-3 bond in 3^{**} does not affect $d_{C-2-C-3}$ very much; $d_{C-2-C-3}$ is suggested to essentially have normal C-C single bond character. Furthermore, judging from the calculated potential energy (E) of 3^{**} along the θ (therefore, C-2-C-3 is torsional) coordinate (Figure 4), the rotation barrier is less than 6 kcal mol⁻¹ at $\theta \approx +90^\circ$, which corresponds to that (3–6 kcal mol⁻¹) of the normal C-C single bond, indicating that the C-2-C-3 bond of 3^{**} does not have the typical nature of a double bond.¹⁸ These findings suggest that the ground state of 3^{**} is nearly planar, but possesses an electronic state that is considerably localized in subunits I and II, as depicted in 3^{*np} in Scheme 1, supporting the proposal based on the absorption and emission analyses.

The electronic transition wavelengths (λ_{et}) and oscillator strengths (f) of 3^{**} and 7^{\bullet} in the optimized structures were calculated with TD-UB3LYP/cc-pVDZ and are summarized in Table 1. The calculated λ_{et} at 303 and 323 nm, with $f_A = 0.25$ and $f_B = 0.21$ for 3^{**} , are in good agreement with the observed λ_{ab} at 298 and 328 nm of bands A and B, respectively (Figure 1). Similarly, the 327-nm transition with $f = 0.46$, calculated as the λ_{et} of 7^{\bullet} , is in line with the observed 336-nm absorption band (Figure 2). Although two weak absorption bands with λ_{ab} at 448 and 472 nm (band C) of 3^{**} were not reproduced by the calculation at this level, it is evident that these bands and bands A and B originate from the same species, 3^{**} . The corresponding absorption bands with λ_{ab} at 488 and 518 nm of 7^{\bullet} were similarly not reproduced by the calculation. These irreproducible bands are probably due to forbidden transitions. The calculated electronic transitions of 3^{**} (Figure 6) successfully reproduced the observed absorption spectra of 3^{**} (Figure 1) except for forbidden transitions, resulting in the same conclusion as that from the absorption and emission analyses.

Figure 7a shows the molecular orbitals (MOs) associated with the calculated transition for bands A and B of

(16) Interestingly, the bond length, $d_{C-2-C-3} = 1.44(2)$ Å, of 3^{**} at $\theta = 0^\circ$ is longer by 0.03 Å than that (1.41 Å) of a structurally related but nonarylated 14^{*p} with planar geometry ($\theta = 0^\circ$, Chart 2), indicating that substitution of two phenyl groups induces elongation of the C-2-C-3 bond, which is probably due to the essentially localized electronic state.

(17) Krylov, A. I.; Sherrill, C. D. *J. Chem. Phys.* **2002**, *116*, 3194–3203.

(18) One of the reviewer suggests that these findings are consistent with previous observations made by Berson¹⁹ and Little²⁰ in cycloadditions of other TMMs.

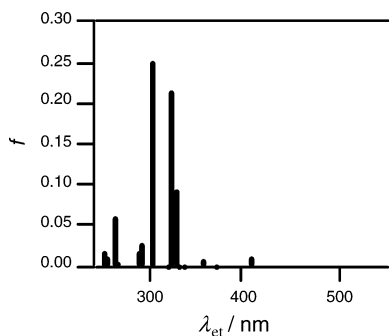


FIGURE 6. Electronic transitions of **3**** calculated by TD-UB3LYP/cc-pVDZ.

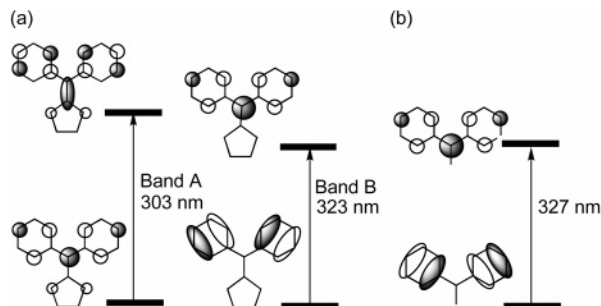


FIGURE 7. Schematic representation of the MOs of (a) **3**** and (b) **7*** associated with bands A and B. The calculated wavelengths are shown.

3.** The MOs for band B (calculated 323 nm, experimental 328 nm) possess orbital coefficients only in subunit I; their pattern bears a close resemblance to that of the transition of **7*** (Figure 7b) (calculated 327 nm, experimental 336 nm). This is in accord with the finding that band B corresponds to the 336-nm transition of **7*** in the spectra. On the other hand, Figure 7a shows that the transition of band A induces an increment of bond order of the C-2–C-3 bond; note that orbital coefficients appear at C-2 and C-3 with a synchronous phase combination after the transition. These results are reasonable because **7***, without the C-2–C-3 bond of **3****, has neither an absorption band nor an oscillator strength corresponding to those of band A. Consequently, the electronic transition involved with both subunits I and II is most likely responsible for absorption band A.

Next, we examined the dihedral angle (θ)-dependent changes of the oscillator strengths (f_A and f_B) for bands A and B of **3**** using TD-DFT calculations, as shown in Figure 8. According to the changes in θ from 0° to $+90^\circ$, f_A increased to reach a maximum at $\theta \approx +10$ – 20° , and then decreased monotonically. This is relevant to the decrement of the orbital overlap at C-2 and C-3 in the excited state of **3**** associated with band A. On the other hand, f_B reached a maximum at $\theta \approx +50$ – 60° . Figure 8 indicates that band A would not be observed if **3**** were completely bisected ($\theta = \pm 90^\circ$). A combination of the calculation and the finding that band A is observed with considerable intensity (Figure 1) implies that **3**** is nearly planar, rather than bisected or largely twisted, as shown for **3**_{np}** in Scheme 1.

Conversely, the real θ of **3**** can be estimated from the relationship between θ and the f -value ratio, f_B/f_A (Figure 9), and the observed spectra (Figure 1). Note that the

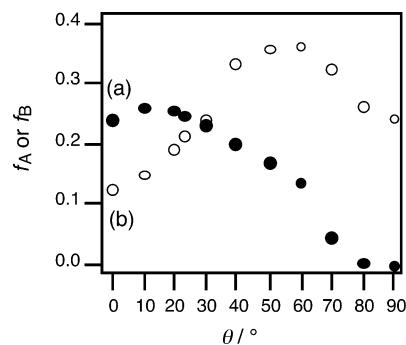


FIGURE 8. Dihedral angle (θ)-dependent changes of the oscillator strengths [(a) f_A and (b) f_B] for absorption bands A and B of **3****, calculated by TD-UB3LYP/cc-pVDZ.

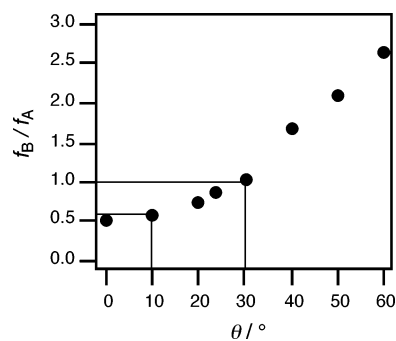


FIGURE 9. Relationship between θ and the f -value ratio, f_B/f_A .

area (S) ratio of bands A and B, S_B/S_A , should correspond to f_B/f_A . The value $S_B/S_A = 0.8 \pm 0.2$, obtained from the absorption spectra of **3**** (Figure 1), agrees favorably with $f_B/f_A = 0.84$ (Table 1), and further suggests $\theta = +20 \pm 10^\circ$ in Figure 9, showing an excellent coincidence with the conclusion from the DFT calculations ($\theta = +23.5^\circ$). These findings indicate that the DFT and TD-DFT calculations used here are reliable tools for exploring the molecular geometry and electronic structure of the ground state of **3****.

Comparison of the calculated singlet–triplet gap ($\Delta E = E_S - E_T$) between **3**** and related TMMs is of interest and supports the proposal for the molecular geometry and electronic structure of **3****. ΔE of **3**** was calculated to be ca. 21.2 kcal mol⁻¹ by DFT calculation (UB3LYP/cc-pVDZ). The ground-state triplet ($\theta = +23.5^\circ$) and singlet ($\theta = +55.2^\circ$) of **3**** may be comparable to the ground-state triplet (${}^3A'_2$, $\theta = 0.0^\circ$) and singlet (1B_1 , $\theta = +90.0^\circ$) of the parent TMM, **1***, respectively. According to Cramer's calculations based on multiconfiguration self-consistent-field followed by multireference second-order perturbation theory and DFT, ΔE of **1*** is 14.7–16.9 kcal mol⁻¹.²¹ ΔE of the methylenecyclopentane-2,5-diyl (**14**_p**, Chart 2) was calculated to be 9.53 kcal mol⁻¹. Moreover, ΔE of the isopropylidenecyclopentane-2,5-diyl (**15**_p**) was estimated to be at least 13 and 11.7 kcal mol⁻¹ by Berson²² and Platz,^{6e} respectively. Although ΔE of **3**** is somewhat

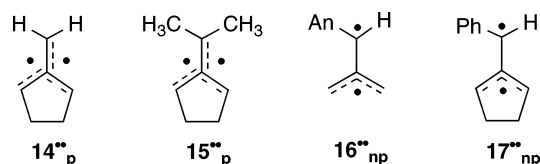
(19) Siemionko, R. K.; Berson, J. A. *J. Am. Chem. Soc.* **1980**, *102*, 3870–3882 and references therein.

(20) Stone, K. J.; Little, R. D. *J. Am. Chem. Soc.* **1985**, *107*, 2495–2505 and references therein.

(21) Cramer, C. J.; Smith, B. A. *J. Phys. Chem.* **1996**, *100*, 9664–9670.

(22) Mazur, M. R.; Berson, J. A. *J. Am. Chem. Soc.* **1982**, *104*, 2217–2222.

CHART 2



larger than those of 1^{**} , 14^{**}_p , and 15^{**}_p , it is clear that this value is consistent with a single molecular species postulate that requires large ΔE .

Substituent Effects on the UV/VIS Absorption and Emission Spectra of 3^{} .** If the proposal described above is correct, regiospecific substituent effects on UV/VIS absorption and emission spectra should be observed when subunits I and II are substituted independently. To test this, we examined the UV/VIS absorption and emission spectra of TMMs 11^{**} and 13^{**} using the photo-reactions of diazene **10** and quadricyclane **12**,¹² respectively. TMMs 11^{**} and 13^{**} represent a 4,4'-dimethoxy derivative of the two phenyl groups in subunit I, and a cyclobutene-fused derivative of subunit II, in 3^{**} , respectively (Scheme 1). TMM diradical 11^{**} had absorption bands with λ_{ab} at 314, 346, and 494 nm and emission bands with λ_{em} at ca. 510 nm¹⁵ (shoulder), which correspond to bands A, B, C, and D of 3^{**} , respectively (Table 1). Similar absorption bands with λ_{ab} at 310, 328, and 472 nm and emission bands with λ_{em} at 488 nm were observed for 13^{**} . As shown in Table 1, all the absorption and emission bands of 11^{**} were red-shifted, compared with that of 3^{**} , while a similar red-shift in 13^{**} was observed only for the absorption band with λ_{ab} at 310 nm, which corresponds to band A of 3^{**} with λ_{ab} at 298 nm. These findings indicate that subunits I and II both affect band A, while only subunit I affects the other bands (B, C, and D). Therefore, the experimental substituent effects are in line with the calculation and further support the evolved explanation.

Comparison of 3^{}_{np} with Structurally Related TMMs.** It is of interest to compare 3^{**}_{np} with 5^{**}_{lt} , which are similarly diaryl-substituted, but are five-membered cyclic and acyclic TMMs, respectively; 3^{**}_{np} is suggested to be nearly planar ($\theta = +23.5^\circ$), while 5^{**}_{lt} is largely twisted^{7c} ($\theta = +32.1^\circ$). This contrast must be due to the difference between 3^{**}_{np} and 5^{**}_{lt} in the degree of steric interaction between the two aryl moieties and the allyl radical moiety. Note that a change in structure from acyclic 5^{**}_{lt} to five-membered cyclic 3^{**}_{np} reduces the interior angle of the allyl radical part from ca. 120° to ca. 108° and, accordingly, the steric interaction.

This is also reasonable from the point of view of the values of the zero-field splitting parameter, $|D/hc|$. As shown in Chart 2 and Table 2, $|D/hc|$ decreases with aryl substitutions in both acyclic (1^{**}_p , 16^{**}_{np} , and 5^{**}_{lt}) and five-membered cyclic (14^{**}_p , 17^{**}_{np} , and 3^{**}_{np}) TMMs. These aryl substitution effects on $|D/hc|$ are in accord with a simple prediction from a theoretical approximation (eq 1),²⁴ where ρ_A and ρ_B are spin densities at C-1 and C-3, respectively, and d is the distance between two unpaired

electrons (A and B). Note that ρ decreases with aryl substitution(s) due to spin delocalization on aryl group(s), whereas d increases with increasing θ .

$$|D/hc| = \frac{3\mu_0 g^2 \mu_B^2 \rho_A \rho_B}{16\pi d^3} \quad (1)$$

The differential values, $|\Delta_\theta|$ and Δ_D , which are defined in Table 2, lead us to compare the degree of the aryl substitution effects between the acyclic and cyclic series. Comparing the parent systems (1^{**}_p and 14^{**}_p), a systematic difference ($\Delta_D = 0.0025 \text{ cm}^{-1}$) in $|D/hc|$ between the acyclic and cyclic series is evident. Larger Δ_D values are induced by aryl ($\Delta_D = 0.0046 \text{ cm}^{-1}$ for the aryl system²⁵) and diaryl ($\Delta_D = 0.0064 \text{ cm}^{-1}$ for the diaryl system²⁵) substitutions. Δ_D is closely linked with increasing d via increasing $|\Delta_\theta|$, as well as decreasing ρ . In evaluating d , it is hard to separate the effects of the steric interaction and those of aryl-induced spin delocalization; they work in close cooperation. However, judging from the difference in $|D/hc|$ between acyclic and cyclic TMMs (16^{**}_{np} vs 17^{**}_{np} or 5^{**}_{lt} vs 3^{**}_{np}), it is likely that the steric interaction is one of the important factors. Therefore, the findings described above indicate that the steric interaction in the cyclic 3^{**}_{np} is relieved by the five-membered cyclic structure, as compared with acyclic 5^{**}_{lt} .

Conclusion

We propose that triplet TMM 3^{**} in a low-temperature matrix is not planar as previously believed, but adopts a nearly planar conformation, as shown in 3^{**}_{np} in Scheme 1.²⁶ Its electronic structure is the considerably localized electronic state. This is the first proposal based on a comparison of the absorption and emission spectra of TMM 3^{**} with those of **7** and **9**. A DFT calculation confirmed the molecular geometry ($\theta = +23.5^\circ$) and electronic structure of 3^{**} . A TD-DFT calculation of 3^{**} , the first application to TMM systems, reproduced the observed spectrum.²⁸ The substituent effects on the absorption and emission spectra of 3^{**} using 11^{**} and 13^{**} support the evolved explanation. This proposal does not mean that an electronic interaction between subunits I and II is completely broken. In fact, band A involves a strong electronic interaction between the two, especially in the excited state, as shown in the text. In addition, as

(25) A comparison of $|D/hc|$ of phenyl (17^{**}_{np} or 3^{**}_{np}) and 4-methoxyphenyl (16^{**}_{np} or 5^{**}_{lt}) derivatives is appropriate, because no significant substituent effects on $|D/hc|$ were observed between 17^{**}_{np} and the corresponding 4-methoxyphenyl derivatives.^{9b}

(26) Wirtz et al. raised an objection to the two molecular species postulate based on semiempirical calculation results.²⁷ They suggested that trace impurities formed in the photoreaction of diazene **2** were the origin of weak absorption band C and emission band D. By contrast, we believe that bands C and D arose from the sole species 3^{**} , because similar bands were observed for diradical 13^{**} and radical **7**, which were independently generated from quadricyclane **12** and alcohol **6**, respectively, but not from diazene precursors. In addition, samples **2**, **6**, **10**, and **12** gave satisfactory elemental analyses (within 0.4%). Wirtz et al. also pointed out that more work was needed to establish the UV/VIS absorption spectra of TMMs, including 3^{**} , and this was also one of the factors motivating our work.

(27) Gisin, M.; Wirtz, J. *Helv. Chim. Acta* **1983**, *66*, 1556–1568.

(28) Careful analyses are needed for the MO calculations of the excited states of open-shell systems, because they can give misleading results.²⁹ This is why we not only analyzed the absorption spectrum with DFT calculations, but also compared the absorption and emission spectra with those of the TMM diradicals 11^{**} and 13^{**} and related radicals **7** and **9**.

(23) (a) Dowd, P. *Acc. Chem. Res.* **1972**, *5*, 242–248. (b) Dixon, D. A.; Dunning, T. H., Jr.; Eades, R. A.; Kleier, D. A. *J. Am. Chem. Soc.* **1981**, *103*, 2878–2880.

(24) Adam, W.; Kita, F.; Harrer, H. M.; Nau, W. M.; Zipf, R. *J. Org. Chem.* **1996**, *61*, 7056–7065 and references therein.

TABLE 2. Dihedral Angles (θ) and $|D/hc|$ Values of Acyclic and Cyclic TMMs

	acyclic			cyclic			$ \Delta_\theta ^b/\text{deg}$	$\Delta_D^c/\text{cm}^{-1}$
	TMMs	θ^a/deg	$ D/hc /\text{cm}^{-1}$	TMMs	θ^a/deg	$ D/hc /\text{cm}^{-1}$		
parent	1^{••}_p	0	0.024 ^d	14^{••}_p	0	0.0265 ^e	0	0.0025
aryl	16^{••}_{np}	+17.4	0.015 ^f	17^{••}_{np}	+13.2	0.0196 ^e	4.2	0.0046
diaryl	5^{••}_{it}	+32.1	0.0116 ^f	3^{••}_{np}	+23.5	0.0180 ^e	8.6	0.0064

^a Calculations were carried out with UB3LYP/cc-pVDZ. ^b $|\Delta_\theta| = |\theta(\text{cyclic}) - \theta(\text{acyclic})|$. ^c $\Delta_D = |D/hc|(\text{cyclic}) - |D/hc|(\text{acyclic})$. ^d See refs 3 and 23. ^e See ref 4b. ^f See ref 7c.

Berson and co-workers pointed out, a change in the conformation of **3^{••}** by bond rotations is possible in a solution. Therefore, the proposal is applied to **3^{••}** only in a low-temperature matrix, but does not always apply to **3^{••}** in a solution.³⁰

The present work is not consistent with the presence of two molecular species in equilibrium as initially postulated (and later corrected), but is most consistent with the presence of a single molecular species, the nearly planar triplet TMM, **3^{••}_{np}**. However, this work does not deny the contribution of Berson and co-workers.^{4c} On the contrary, this work may correspond to the extension of another postulate, their single molecular species postulate (see Introduction). Namely, our proposal is a much-clarified version of the original explanation by them. Their analysis was based on the assumption that the singlet–triplet energy gap ΔE of **3^{••}** corresponds to that (<3.5 kcal mol⁻¹) of **15^{••}_p**.³¹ Later studies of the Berson group^{1c,d,22} and calculations of Auster, Pitzer, and Platz^{6e} led to a question of their original conclusion of a small ΔE in TMMs. The revised estimates of the ΔE for **15^{••}_p**, >13 and >11.7 kcal mol⁻¹ by Berson²² and Platz,^{6e} respectively, are in good agreement with the recent spectroscopic determination for the parent TMM by Squires et al.³² $\Delta E = 15$ kcal mol⁻¹. If they had been aware of the large ΔE value, they might have proposed another interpretation, probably the single molecular species postulate.³³

Anyhow, in this work, a comparison of the absorption and emission wavelengths and the $|D/hc|$ values of **3^{••}_{np}** with those of the related TMM diradicals revealed that the molecular geometry and the electronic structure of TMMs strongly depend on the number of aryl groups and their cyclic structures. Our results provide meaningful information not only for pure TMM chemistry,³⁴ but also for the molecular design of TMMs for many applications, such as in organic syntheses^{1e,f,35} and molecular devices, where the TMM framework is used as a building block of functionalized organic materials.³⁶

(29) Borden, W. T.; Iwamura, H.; Berson, J. A. *Acc. Chem. Res.* **1994**, *27*, 109–116.

(30) As one of the reviewers stressed, a spectroscopically undetectable amount of largely twisted TMMs could be a critical reactive species in trapping experiment in solution. We think that more work is needed to establish the reactivity of TMMs in solution.

(31) Platz, M. S.; Berson, J. A. *J. Am. Chem. Soc.* **1977**, *99*, 5178–5180.

(32) Wenthold, P. G.; Hu, J.; Squires, R. R.; Lineberger, W. C. *J. Am. Chem. Soc.* **1996**, *118*, 475–476.

(33) For further discussion, see refs 1c and 1d.

(34) For example, the results will provide meaningful information on the problem of the difficulty in simulating the $|D/hc|$ value of various TMMs.

(35) (a) Trost, B. M. *Angew. Chem., Int. Ed. Engl.* **1986**, *25*, 1–20. (b) Maiti, A.; Gerken, J. B.; Masjedizadeh, M. R.; Mimieux, Y. S.; Little, R. D. *J. Org. Chem.* **2004**, *69*, 8574–8582.

Experimental Section

General Method. See the Supporting Information.

Syntheses. Diazene **2** was prepared by the reduction of diethyl 7-(diphenylmethylene)-2,3-diazabicyclo[2.2.1]heptane-2,3-dicarboxylate, which was obtained by the Diels–Alder reaction of diphenylfulvene with diethyl azodicarboxylate, followed by hydrogenation, slightly modifying the method reported previously.³⁷ The diazene **10** was similarly obtained by using bis(4-methoxyphenyl)fulvene.³⁸ Diphenylethanol **6**³⁹ was obtained by the Grignard reaction of benzophenone with methyl iodide. Bromocyclopentene **8** was prepared by the bromination of cyclopentene with *N*-bromosuccinimide as reported previously.⁴⁰ Quadricyclane **12**^{12a} was prepared by the Peterson reaction⁴¹ with use of quadricyclanone⁴² and benzhydryltrimethylsilane.⁴³ Physical data on the key compounds are given in the Supporting Information.

Measuring the Absorption and Emission Spectra during Photoreaction in a Glassy Matrix. The general procedure was as follows. A MCH solution (1 mL) containing substrate (1.0 mM for **2**, 0.2 mM for **10** and **12**) in a flat vessel (synthetic quartz, 2 × 10 × 40 mm³ thickness × width × height) was degassed by 5 freeze (77 K)–pump (10⁻² Torr)–thaw (ambient temperature) cycles, and then sealed at 10⁻² Torr at 77 K in the dark. A glassy matrix was obtained by steeping the vessel in liquid nitrogen. This vessel was irradiated with a lamp (2537 Å, 15 W) for several minutes in liquid nitrogen at 77 K. The absorption spectra changes during the photoreaction were observed at 77 K with an absorption spectrophotometer. Similarly, the emission spectra were recorded with a fluorescence spectrophotometer (e.g., $\lambda_{\text{ex}} = 328$ nm, band-pass 5 nm for **3^{••}**). See the Supporting Information for the UV/VIS absorption and emission spectra of **11^{••}** and **13^{••}**.

Measuring the Absorption and Emission Spectra of a γ -Ray Irradiated Glassy Matrix. A MCH solution (1 mL) containing **6** (10 mM) or **8** (10 mM) in a flat vessel (synthetic quartz, 2 × 10 × 40 mm³ thickness × width × height) was separately degassed by 5 freeze (77 K)–pump (10⁻² Torr)–thaw (ambient temperature) cycles, and then sealed at 10⁻² Torr. A glassy matrix was obtained by steeping the vessel into liquid nitrogen. This vessel was irradiated with γ -ray from a 5.1 TBq ⁶⁰Co source in liquid nitrogen at 77 K for 16 h. The absorption spectra changes before and after irradiation were

(36) (a) Dougherty, D. A. *Acc. Chem. Res.* **1991**, *24*, 88–94. (b) Matsumoto, T.; Ishida, T.; Koga, N.; Iwamura, H. *J. Am. Chem. Soc.* **1992**, *114*, 9952–9959. (c) Jacobs, S. J.; Shultz, D. A.; Jain, R.; Novak, J.; Dougherty, D. A. *J. Am. Chem. Soc.* **1993**, *115*, 1744–1753. (d) Bregant, T. M.; Groppe, J.; Little, R. D. *J. Am. Chem. Soc.* **1994**, *116*, 3635–3636.

(37) Adam, W.; Finzel, R. *J. Am. Chem. Soc.* **1992**, *114*, 4563–4568.

(38) Jeffery, J.; Probitts, E. J.; Mawby, R. J. *J. Chem. Soc., Dalton Trans.* **1984**, *11*, 2423–2427.

(39) Kharasch, M. S.; Lambert, F. L. *J. Am. Chem. Soc.* **1941**, *63*, 2315–2316.

(40) Ford, M. C.; Waters, W. A. *J. Chem. Soc. Abstr.* **1952**, 2240–2245.

(41) Hudrlik, P. F.; Peterson, D. *J. Am. Chem. Soc.* **1975**, *97*, 1464–1468.

(42) Hoffmann, R. W.; Hirsch, R. *Liebigs Ann. Chem.* **1969**, 727, 222–223.

(43) Hill, M. S.; Hitchcock, P. B. *Organometallics* **2002**, *21*, 220–225.

observed at 77 K with an absorption spectrophotometer. Similarly, the emission spectra were recorded with a fluorescence spectrophotometer (e.g., $\lambda_{\text{ex}} = 336$ nm, band-pass 5 nm for **7**^{*}).

Quantum Chemical Calculations. DFT and TD-DFT calculations were performed with the program Gaussian 98.⁴⁴ Figure 3a was drawn with use of the MOLEKEL software.⁴⁵ The Cartesian coordinates for the optimized structures of **1**^{*}_p,

(44) Frisch, M. J.; Trucks, G. W.; Schlegel, H. B.; Scuseria, G. E.; Robb, M. A.; Cheeseman, J. R.; Zakrzewski, V. G.; Montgomery, J. A.; Stratmann, R. E.; Burant, J. C.; Dapprich, S.; Millam, J. M.; Daniels, A. D.; Kudin, K. N.; Strain, M. C.; Farkas, O.; Tomasi, J.; Barone, V.; Cossi, M.; Cammi, R.; Mennucci, B.; Pomelli, C.; Adamo, C.; Clifford, S.; Ochterski, J.; Petersson, G. A.; Ayala, P. Y.; Cui, Q.; Morokuma, K.; Malick, D. K.; Rabuck, A. D.; Raghavachari, K.; Foresman, J. B.; Cioslowski, J.; Ortiz, J. V.; Stefanov, B. B.; Liu, G.; Liashenko, A.; Piskorz, P.; Komaromi, I.; Gomperts, R.; Martin, R. L.; Fox, D. J.; Keith, T.; Al-Laham, M. A.; Peng, C. Y.; Nanayakkara, A.; Gonzalez, C.; Challacombe, M.; Gill, P. M. W.; Johnson, B. G.; Chen, W.; Wong, M. W.; Andres, J. L.; Head-Gordon, M.; Replogle, E. S.; Pople, J. A. *Gaussian 98*, Revision A.11.4; Gaussian, Inc.: Pittsburgh, PA, 1998.

(45) Flukiger, P.; Luthi, H. P.; Portmann, S.; Weber, J. *MOLEKEL 4.3*; Swiss Center for Scientific Computing: Manno, Switzerland, 2002.

3^{*}_{np}, **5**^{*}_{lt}, **14**^{*}_p, **16**^{*}_{np}, and **17**^{*}_{np} are given in the Supporting Information.

Acknowledgment. H.I. acknowledges the Ministry of Education, Culture, Sports, Science, and Technology of Japan for financial support in the form of a Grant-in-Aid for Scientific Research in Priority Areas (Area No. 417) and others (Nos. 122440173 and 14050008). We also thank Professors J. A. Berson (Yale University), M. S. Platz (Ohio State University), N. J. Turro (Columbia University), K. Akiyama (Tohoku University), and T. Hirano (The University of Electro-Communications) for their valuable discussions and Professor M. Ueda (Tohoku University) for his generous support.

Supporting Information Available: The general method of the experiments, spectroscopic data for key compounds, UV/VIS absorption and emission spectra of TMMs (**11**^{*} and **13**^{*}), and the Cartesian coordinates of TMMs optimized by DFT calculations. This material is available free of charge via the Internet at <http://pubs.acs.org>.

JO047893O